

# ChemComm

Accepted Manuscript



This is an *Accepted Manuscript*, which has been through the Royal Society of Chemistry peer review process and has been accepted for publication.

*Accepted Manuscripts* are published online shortly after acceptance, before technical editing, formatting and proof reading. Using this free service, authors can make their results available to the community, in citable form, before we publish the edited article. We will replace this *Accepted Manuscript* with the edited and formatted *Advance Article* as soon as it is available.

You can find more information about *Accepted Manuscripts* in the [Information for Authors](#).

Please note that technical editing may introduce minor changes to the text and/or graphics, which may alter content. The journal's standard [Terms & Conditions](#) and the [Ethical guidelines](#) still apply. In no event shall the Royal Society of Chemistry be held responsible for any errors or omissions in this *Accepted Manuscript* or any consequences arising from the use of any information it contains.

Cite this: DOI: 10.1039/c0xx00000x

www.rsc.org/xxxxxx

ARTICLE TYPE

# Multifunctional Upconverting Nanoparticles for Near-Infrared Triggered and Synergistic Antibacterial Resistance Therapy

Meili Yin<sup>a</sup>, Zhenhua Li<sup>ab</sup>, Enguo Ju<sup>ab</sup>, Zhenzhen Wang<sup>ab</sup>, Kai Dong<sup>ab</sup>, Jinsong Ren<sup>a\*</sup> and Xiaogang Qu<sup>a\*</sup>

Received (in XXX, XXX) Xth XXXXXXXXXX 20XX, Accepted Xth XXXXXXXXXX 20XX

DOI: 10.1039/b000000x

To integrate photodynamic therapy with photothermal therapy for improved multidrug-resistant bacteria therapy, we constructed a novel multifunctional core/satellite nanostructure by decorating CuS nanoparticles onto the surface of NaYF<sub>4</sub>:Mn/Yb/Er@photosensitizer doped SiO<sub>2</sub>. This system exhibited a superior antibacterial activity towards drug-resistant *Staphylococcus aureus* and *Escherichia coli*.

In the last few decades, antibiotics have been used very intensively and conventional antibiotic therapies were becoming less efficient owing to the emergence of antibiotic-resistant bacterial strains.<sup>[1]</sup> Drug resistance enforces high-dose administration of antibiotics, often generating intolerable toxicity. The demand of developing new antibiotics and therapies for combating bacterial infections is becoming crucial. Recent advances in nanotechnology have provided the potential for using inorganic nanoparticles and semiconductors in the fight against multidrug-resistant bacteria.<sup>[2]</sup> For example, gold NPs and graphene, which have strong light-absorbing, had been widely developed as photothermal therapy (PTT) materials to destroy bacteria by combining pulsed laser.<sup>[3]</sup> Meanwhile, photodynamic therapy (PDT) has been proposed as an alternative bactericidal method to combat antibiotic-resistant pathogenic microbes.<sup>[4]</sup> Functionalized magnetic particles with photosensitizers (PS) for pathogenic bacteria therapy had been reported.<sup>[5]</sup> However, their photodynamic effect was still inadequate to gram-negative bacteria. Multimodal therapy, the synergistic or combined effect of two different therapeutic modalities, has become a promising approach to enhance antibacterial therapy.<sup>[3e,5]</sup> Nevertheless, the synergistic antibacterial resistance therapy combining the advantage of PDT/PTT has not yet been well explored.

Semiconductor CuS nanoparticles are a new class of photothermal agents that provide an alternative to gold analogues.<sup>[6]</sup> Gold nanostructures such as gold nanorods, are widely used as PTT agents, which would “melt” and lose their NIR absorbance after being irradiated by the laser over a certain period of time. Contrast to gold nanostructures, CuS exhibit great photostability without any significant decrease in optical absorbance even after laser exposure for a long time. Additionally, CuS nanoparticles are irradiated with a 980 nm laser for the photothermal conversion, which shows deeper penetration in biological tissues and enhanced photothermal ablation efficiency. Recently, upconverting nanoparticles (UCNPs), which are able to

absorb NIR light and convert it into high-energy photons in a very broad range from the UV to the NIR region, have emerged as an appealing candidate for the application of NIR-induced mediator.<sup>[7]</sup> The therapeutic efficiency of conventional PDT relies on the light and PS delivery to oxygenated tissues, which, unfortunately, suffers greatly from the very limited depth of penetration (less than 2 mm) of visible light.<sup>[4a]</sup> UCNPs have been used as nanotransducers to fabricate UCNP/PS nanostructures for solving the problems that traditional PDT has faced.<sup>[8]</sup> Otherwise, UCNPs have attracted increasing attention due to their general features that include excellent photostability, high brightness under low-power continuous-wave laser excitation and deep penetration into biological systems and relatively low toxicity.<sup>[7,8]</sup> Here for the first time, we synthesized a novel multifunctionalized UCNPs for synergistic PDT/PTT antibacterial resistance therapy. As illustrated in Fig. 1a, UCNPs were covered by Methylene blue (MB) doped silica (UCNPs/MB). To improve the effective of efficient energy transfer from UCNPs to MB, the pure dark red emission (650-670nm) of NaYF<sub>4</sub>:Mn/Yb/Er had been synthesized.<sup>[9]</sup> By incorporating CuS on nanostructures (UCNPs/MB/CuS), we had combined PDT with PTT to obtain high therapeutic index via synergistic effect. Chitosan (Cis) was finally grafted to prevent aggregations among the particles and impart excellent water-solubility and biocompatibility.

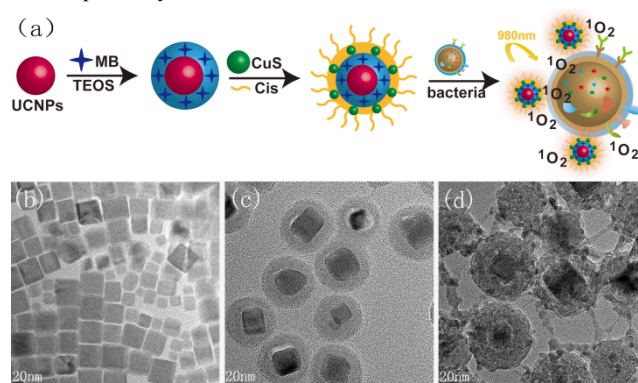


Fig. 1 Schematic illustration of the construction of UCNPs/MB/CuS-Cis as a multifunctional system for PDT/PTT synergistic therapy of bacteria (a) and morphology and crystal structure of the NaYF<sub>4</sub>:Mn/Yb/Er (b), UCNPs/MB-NH<sub>2</sub> (c) and UCNPs/MB/CuS-Cis nanoparticles (d).

NaYF<sub>4</sub>:Mn/Yb/Er (30:18:2 mol%) was prepared by using previously reported procedures.<sup>[9]</sup> As indicated in the

transmission electron microscopy (TEM) images, the products obtained after each synthetic step show an excellent dispersity and uniformity in both morphology and dimension with an ultimate average diameter of 60 nm (Fig. 1b-d and Fig. S1). The core-satellite structure could be clearly seen in the TEM and scanning electron microscopy images (SEM) (Fig. S1b). Energy dispersive spectroscopic (EDS) element analysis of Y, Mn, Yb, Er, F, S and Cu were further performed to investigate the distribution of various components (Fig. S2). Particle size distribution analysis was used to confirm the monodisperse property of nanoparticles (Fig. S3). The successful adsorption of Cis was confirmed by FTIR spectroscopy and zeta potential analysis (Fig. S4).

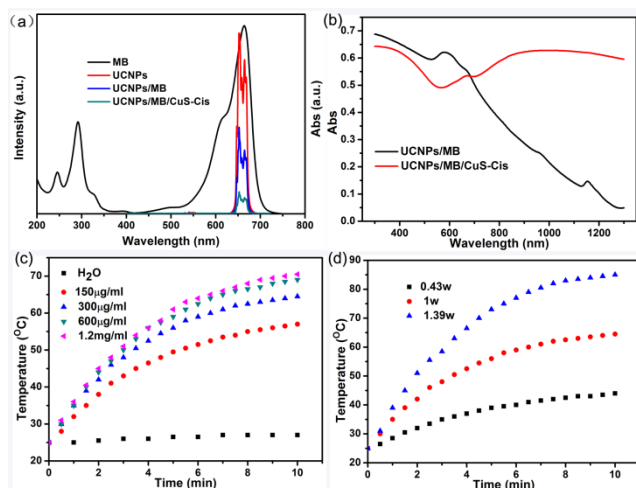


Fig. 2 (a) The emission spectra of UCNPs, UCNPs/MB-NH<sub>2</sub> and UCNPs/MB/CuS-Cis and the absorption spectra of MB. (b) UV-Vis-NIR absorption spectra of the UCNPs/MB-NH<sub>2</sub> and UCNPs/MB/CuS-Cis. NIR-induced heat generation of UCNPs/MB/CuS-Cis aqueous solution (c) different concentrations at the same power density of 1 W cm<sup>-2</sup> and (d) 300 μg ml<sup>-1</sup> at different power densities.

For NIR-laser-triggered PDT, MB was selected in this study due to its well-matched absorption with NaYF<sub>4</sub>:Mn/Yb/Er emission. Fig. 2a clearly showed the spectra overlap between MB absorption (654 nm) and NaYF<sub>4</sub>:Mn/Yb/Er red emission peak (651 nm). Because the surrounding MB and CuS blocked the emissions to some extent, the fluorescent intensities of the upconverting nanoparticles at emission peaks of 650-670 nm were gradually lowered. Generation of <sup>1</sup>O<sub>2</sub> by these UCNP-based photosensitizers was detected chemically, using 1,3-diphenylisobenzofuran (DPBF) as a <sup>1</sup>O<sub>2</sub> sensor.<sup>[10]</sup> As illustrated in Fig. S5, under UCNPs/MB or UCNPs/MB/CuS-Cis exposed to a 980 nm laser, a clear decrease of about 400 nm in the absorption intensity of DPBF took place, which demonstrating that <sup>1</sup>O<sub>2</sub> could be generated. In contrast, no detectable bleaching of the DPBF absorption at 400 nm was observed without 980nm irradiation, which indicating that no <sup>1</sup>O<sub>2</sub> was generated in UCNPs/MB or UCNPs/MB/CuS-Cis.

The optical property of the aqueous dispersion containing 50 μg ml<sup>-1</sup> UCNPs/MB/CuS-Cis nanoconstruction was studied by using UV-Vis-NIR spectroscopy (Fig. 2b). The spectrum was consistent with previous reports.<sup>[6a]</sup> Importantly, UCNPs/MB/CuS-Cis showed an increased absorption with the increase of wavelength in the NIR region (λ = 700-1100 nm),

which motivated us to investigate their potential in PTT therapy of bacteria with a 980 nm laser. Temperature trends of this material were shown in Fig. 2c and 2d, demonstrating that photothermal heating effect could increase monotonically with UCNPs/MB/CuS-Cis concentration and radiant energy. It could be concluded that the CNPs/MB/CuS-Cis nanoconstruction could rapidly convert the 980 nm laser energy into environmental heat. This proved that UCNPs/MB/CuS-Cis was promising as an ideal photothermal converter in antibacterial resistance therapy.

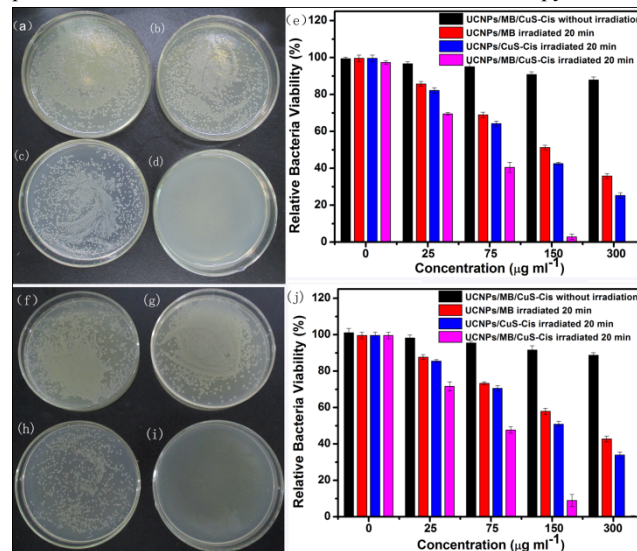


Fig. 3 Photographs of bacterial colonies formed by *S. aureus* (a-d) and *E. coli* (f-i) in the absence of UCNPs/MB/CuS-Cis (a,f), and 980nm irradiated for 20 min treated with 0 μg ml<sup>-1</sup> (b,g), 25 μg ml<sup>-1</sup> (c,h) and 300 μg ml<sup>-1</sup> (d,i) UCNPs/MB/CuS-Cis nanoparticles. Relative bacteria viability of *S. aureus* (e) and *E. coli* (j) treated with UCNPs/MB and UCNPs/MB/CuS-Cis at different concentrations. Power density was 1 W cm<sup>-2</sup> for 20 min.

The antibacterial activity was evaluated by using both gram-positive oxacillin drug-resistant *Staphylococcus aureus* (*S. aureus*) and gram-negative kanamycin drug-resistant *Escherichia coli* (*E. coli*) bacteria as the bacterium models. The antibacterial activity of the as-prepared UCNPs/MB/CuS-Cis composite could be seen from Fig. 3. The control samples in the absence of UCNPs/MB/CuS-Cis were performed. As shown in Fig. 3a and 3f, both bacterial strains had high survival rate. Under NIR laser irradiation, the bacteria survival rate in the absence of photothermal agents was still above 98%, indicating that NIR laser irradiation alone was harm less to both bacterial strains (Figures 3b and 3g). In contrast, the bacteria survival rate in 25 μg ml<sup>-1</sup> (Fig. 3c and 3h) and 300 μg ml<sup>-1</sup> (Fig. 3d and 3i) UCNPs/MB/CuS-Cis solution dramatically decreased upon NIR laser irradiation for 20 min. Furthermore, the dependence of viability of each bacterium on nanocomposite concentration was depicted in Fig. 3e and 3j. Prior to the NIR laser irradiation, another control experiment was conducted by turbidity measurement. First, bacteria treated with UCNPs/MB/CuS-Cis at different dosage level of up to 300 μg ml<sup>-1</sup> was added without exposure to light and bacteria were incubated for 24 h. As illustrated in Fig. 3e and 3j, when the concentration of UCNPs/MB/CuS-Cis was increased to 300 μg ml<sup>-1</sup>, more than 88% bacteria were still viability, which eliminated the possibility of bacterium death due to particle toxicity. Then, the PDT/PTT tests

of UCNPs/MB and UCNPs/MB/CuS-Cis were performed with 980nm light intensity of  $1 \text{ W cm}^{-2}$  for 20 min. The results showed that without CuS, UCNPs/MB generated a relatively low antibacterial activity. In contrast, the antibacterial activity of UCNPs/MB/CuS-Cis to both the bacteria significantly enhanced. The excellent antibacterial capability by UCNPs/MB/CuS-Cis synergistically increased its antibacterial effectiveness, and a rate of up to 99% bacteria killing efficiency was obtained after NIR laser irradiation. The UCNPs/MB/CuS-Cis was a superior PDT/PTT agent for killing both *S. aureus* and *E. coli*. Compared to *E. coli*, more *S. aureus* were killed after PDT, PTT or PDT/PTT treatment. This result was consistent with the previous reports, which found that gram-positive bacteria were more susceptible to the photodynamic effect than gram-negative bacteria. This might be due to resistance of the outer membrane in gram-negative bacteria.<sup>[11,3c]</sup> The Live/Dead bacterial viability assays were further confirmed the effective antibacterial activity (Fig. S6).

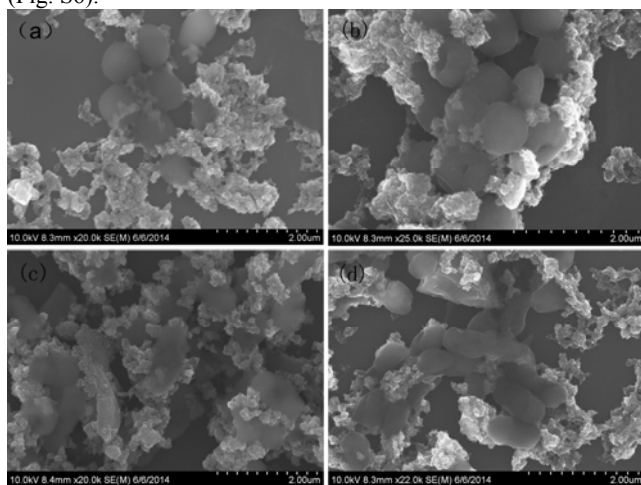


Fig. 4. SEM images of a) *S. aureus* incubated with UCNPs/MB/CuS-Cis, b) *S. aureus* incubated with UCNPs/MB/CuS-Cis under NIR irradiation ; c) *E. coli* incubated with UCNPs/MB/CuS-Cis, d) *E. coli* incubated with UCNPs/MB/CuS-Cis under NIR irradiation.

SEM was used to investigate the morphology change of treated *S. aureus* and *E. coli*. As demonstrated in Fig. 4a, *S. aureus* was a bacteria sphere-shaped and intact surface with the UCNPs/MB/CuS-Cis without NIR laser irradiation. After irradiated, lesions and holes were observed (Fig. 4b). Similarly, *E. coli* was a bacterium with a rod-like shape and intact surface without NIR laser irradiation (Fig. 4c). Distorted and wrinkled membranes were observed in *E. coli* under NIR irradiation (Fig. 4d). While the mechanism of UCNPs/MB/CuS-Cis induced bacteria death was not clearly understood. It has been proposed that cell membrane damage following nanoparticle exposure to NIR radiation could be due to numerous factors, including nanoparticle explosion, shock waves, bubble formation, and thermal disintegration.

## Conclusions

In conclusion, we had constructed a highly efficient NIR photosensitizing nanoplatform for simultaneous PDT/PTT synergistic antibacterial resistance therapy. Our system had the efficient producing of  $^1\text{O}_2$  through the conversion of NIR light to visible

light to activate MB for PDT. CuS nanoparticles were combined with UCNPs/MB to perform the simultaneous PDT/PTT treatment upon single CW laser irradiation. Here, we had demonstrated that our UCNPs/MB/CuS-Cis had the excellent antibacterial efficiency to both gram-positive *S. aureus* and gram-negative *E. coli* bacteria under NIR light. More importantly, compared to PDT or PTT alone, the therapeutic efficacy of UCNPs/MB/CuS-Cis complex was significantly enhanced due to the PDT/PTT synergistic effect.

## Acknowledgements

Financial support was provided by the National Basic Research Program of China (2011CB936004 and 2012CB720602) and the National Natural Science Foundation of China (21301169, 91213302, 21210002).

## Notes and references

- <sup>a</sup> State Key laboratory of Rare Earth Resources Utilization and laboratory of Chemical Biology, Changchun Institute of Applied Chemistry, Chinese Academy of Sciences, Changchun, 130022 P.R. China  
<sup>b</sup> University of Chinese Academy of Sciences, Beijing, 100039 P.R. China  
 E-mail: jren@ciac.ac.cn; xqu@ciac.ac.cn  
 † Electronic Supplementary Information (ESI) available: [details of any supplementary information available should be included here]. See DOI: 10.1039/b000000x/
- [1] J. Davies, D. Davies, *Microbiol. and Mol. Biol. Rev.* 2010, **74**, 417.
  - [2] a) Z. Huang, X. Zheng, D. Yan, G. Yin, X. Liao, Y. Kang, Y. Yao, D. Huang, B. Hao, *Langmuir* 2008, **24**, 4140; b) Z. L. Wang, J. H. Song, *Science* 2006, **312**, 242. c) G. Applerot, A. Lipovsky, R. Dror, N. Perkas, Y. Nitzan, R. Lubart, A. Gedanken, *Adv. Funct. Mater.* **2009**, **19**, 842; b) J. Tian, K. K. Y. Wong, C.-M. Ho, C.-N. Lok, W.-Y. Yu, C.-M. Che, J.-F. Chiu, P. K. H. Tam, *ChemMedChem* **2007**, **2**, 129.
  - [3] a) J. Borovička, W. J. Metheringham, L. A. Madden, C. D. Walton, S. D. Stoyanov, V. N. Paunov, *J. Am. Chem. Soc.* 2013, **135**, 5282; b) W.-C. Huang, P.-J. Tsai, Y.-C. Chen, *Small* **2009**, **5**, 51; c) M.-C. Wu, A. R. Deokar, J.-H. Liao, P.-Y. Shih, Y.-C. Ling, *ACS Nano* 2013, **7**, 1281; d) P. C. Ray, S. A. Khan, A. K. Singh, D. Senapati, Z. Fan, *Chem. Soc. Rev.* 2012, **41**, 3193. e) X. Yang, Z. Li, E. Ju, J. Ren, X. Qu, *Chem. Eur. J.* **2014**, **20**, 394.
  - [4] a) J. P. Celli, B. Q. Spring, I. Rizvi, C. L. Evans, K. S. Samkoe, S. Verma, B. W. Pogue, T. Hasan, *Chem. Rev.* 2010, **110**, 2795; b) C. A. Strassert, M. Otter, R. Q. Albuquerque, A. Höne, Y. Vida, B. Maier, L. De Cola, *Angew. Chem. Int. Ed.* 2009, **48**, 7928.
  - [5] K.-H. Choi, H.-J. Lee, B. J. Park, K.-K. Wang, E. P. Shin, J.-C. Park, Y. K. Kim, M.-K. Oh, Y.-R. Kim, *Chem. Commun.* 2012, **48**, 4591.
  - [6] a) K. Dong, Z. Liu, Z. Li, J. Ren, X. Qu, *Adv. Mater.* 2013, **25**, 4452; b) M. Zhou, R. Zhang, M. Huang, W. Lu, S. Song, M. P. Melancon, M. Tian, D. Liang, C. Li, *J. Am. Chem. Soc.* 2010, **132**, 15351.
  - [7] a) M. K. G. Jayakumar, N. M. Idris, Y. Zhang, *Proc. Natl. Acad. Sci. USA* 2012, **109**, 8483; b) J. Liu, Y. Liu, Q. Liu, C. Li, L. Sun, F. Li, *J. Am. Chem. Soc.* 2011, **133**, 15276; c) C. Wang, H. Tao, L. Cheng, Z. Liu, *Biomaterials* 2011, **32**, 6145; d) Y. Yang, Q. Shao, R. Deng, C. Wang, X. Teng, K. Cheng, Z. Cheng, L. Huang, Z. Liu, X. Liu, B. Xing, *Angew. Chem. Int. Ed.* 2012, **51**, 3125.
  - [8] a) F. Chen, S. Zhang, W. Bu, Y. Chen, Q. Xiao, J. Liu, H. Xing, L. Zhou, W. Peng, J. Shi, *Chem. Eur. J.* 2012, **18**, 7082; b) P. Zhang, W. Steelant, M. Kumar, M. Scholfield, *J. Am. Chem. Soc.* 2007, **129**, 4526.
  - [9] G. Tian, Z. Gu, L. Zhou, W. Yin, X. Liu, L. Yan, S. Jin, W. Ren, G. Xing, S. Li, Y. Zhao, *Adv. Mater.* 2012, **24**, 1226.
  - [10] W. Spiller, H. Kliesch, D. Wöhrle, S. Hackbarth, B. Röder, G. Schnurpfeil, *J. Porphyrins Phthalocyanines* 1998, **2**, 145.
  - [11] P. W. Taylor, P. D. Stapleton, J. Paul Luzio, *Drug Discovery Today* 2002, **7**, 1086.